Journal of Magnetism and Magnetic Materials 323 (2011) 3229–3233

Contents lists available at ScienceDirect

Journal of Magnetism and Magnetic Materials

journal homepage: www.elsevier.com/locate/jmmm

# Magnetocaloric effect at room temperature in manganese perovskite $La_{0.65}Nd_{0.05}Pb_{0.3}MnO_3$ with double resistivity peaks

Zhiming Wang [a,c,*], Qingyu Xu [b], He Zhang [a]

[a] Institute of Mechanical Engineering, Nanjing University of Science and Technology, Nanjing 210094, China
[b] Department of Physics, Southeast University, Nanjing 211189, China
[c] National Laboratory of Solid State Microstructures, Nanjing University, Nanjing 210093, China

ARTICLE INFO

*Article history:*
Received 6 May 2011
Received in revised form
6 July 2011
Available online 21 July 2011

*Keywords:*
Perovskite manganite
Double metal–insulator peak
Magnetocaloric effect at room temperature

ABSTRACT

Series of polycrystalline manganese perovskite oxides $La_{0.7-x}Nd_xPb_{0.3}MnO_3$ ($x=0$, 0.05, and 0.1) are prepared by the sol–gel technique, $La_{0.65}Nd_{0.05}Pb_{0.3}MnO_3$ were representatively investigated because the peculiar double resistivity peaks were found; the maximum magnetic entropy change $\Delta S_H=-2.03$ J/kg K and its good refrigerant capacity 71.05 J/kg around room temperature were obtained under 9 kOe magnetic field variation. The expected double peaks of magnetocaloric effect had not occurred since magnetic entropy change originated from the differential coefficient of magnetic moment to temperature; the relatively well refrigerant capacity possibly results from the faint magnetic inhomogeneity mixed in the double exchange strong magnetic signal.



## 1. Introduction

An intense research effort has recently been devoted to study the interplay between the crystal structure, electrical, magnetic, and thermal properties in the perovskite manganese oxides ($ABO_3$) $A_{1-x}A'_xMnO_3$ ($A^{3+}=La^{3+}$, $Nd^{3+}$, $Pr^{3+}$, $Sm^{3+}$, etc., $A'=Ca^{2+}$, $Sr^{2+}$, $Ba^{2+}$, $Pb^{2+}$, etc.). As a function of temperature, applied magnetic field, and doping, this system displays a rich phase diagram in the magnetotransport and structural properties, for example, the negative colossal magnetoresistance effect (CMR) and the conventionally insulator–metal transition; the latter is generally accompanied by the ferromagnetic order transition [1–8]. Another important physical diagram, the magnetocaloric effect (MC, i.e. the magnetic entropy change), which results from the spin-ordering (i.e. ferromagnetic ordering) and is induced by the variation of the applied magnetic field, is crucial to the technology of magnetic refrigeration with some advantages over gas refrigeration as, low noise, softer vibration, longer usage time, absence of freon, etc. Perovskite manganites, with the same CMR, MC also is often observed around the ferromagnetic ordering transition temperature (i.e. the Curie temperature between a low temperature, metallic–ferromagnetic state and a high temperature, and insulating–paramagnetic state) [9–11], and this evidently suggests that there exists a certain replacing of definite relation between magnetic entropy change and metal–insulator transition of resistivity.

Based on the newly discovered double metal–insulator peaks of resistivity, the aim of this research paper is to search for the possible broad and large refrigerant capacity of magnetocaloric effect in the manganese perovskite at low magnetic fields and in the vicinity of room temperature.

On one hand, the common perovskite manganese oxides are metallic and ferromagnetic at low temperature, while their conductivity displays insulating or semiconducting behavior at high temperature. There is a transition between a metallic–ferromagnetic state at low temperature and an insulating–paramagnetic state at high temperature. The metal–insulator transition of the resistivity between these two states is strongly coupled with the magnetic ordering transition. On the other hand, when a field is applied in the manganese perovskite materials, the unpaired spins are aligned parallel to the field, which lowers the entropy and causes the sample to heat up, on the contrary, when an applied field is removed from a magnetic sample, the spin tends to become random, which increases the entropy and causes the material to cool off. Therefore, the magnetocaloric effect in this kind of material also always occurs at its magnetic ordering transition temperature (i.e. $T_C$).

According to the conventionally double exchange interactional mechanism that involves interaction between pairs of $Mn^{3+}$ and $Mn^{4+}$ ions introduced by Zener in [12], the above-mentioned simultaneous occurrence of ferromagnetism and metallic behavior in manganese perovskite could be explained as reason. In the double exchange model, '$e_g$' electrons can be transferred easily between

* Corresponding author at: Institute of Mechanical Engineering, Nanjing University of Science and Technology, Nanjing 210094, China.
Tel.: +86 25 84318429; fax: +86 25 84315694.
*E-mail address:* zhimingwang@mail.njust.edu.cn (Z. Wang).

0304-8853/$ - see front matter © 2011 Elsevier B.V. All rights reserved.
doi:10.1016/j.jmmm.2011.07.013

ions if the manganese spins are in parallel alignment and are coupled in ferromagnetic, and then the resistivity behavior in some perovskite sample showed a single metal–insulator transition peak. However, it was suggested that the double exchange interactional mechanism alone is not sufficient to explain the details of the observed resistivity behavior such as the insulating behavior above Curie temperature $T_C$, which caused the increase in resistivity as temperature was reduced. The origin of the double metal–insulator transition peaks is still considered an open question and more correlative researches should be carried out to explain this kind of peculiar phenomenon [13–21].

In this paper, we report the magnetocaloric effect of a special perovskite manganite with the double metal–insulator transition peak—$La_{0.65}Nd_{0.05}Pb_{0.3}MnO_3$ at room temperature ($T_C \sim 293$ K).

## 2. Experiments

In the study of manganese perovskite, most endeavors have been concentrated on the doping range $x \sim 1/3$ or 0.3, which is an optimized percentage of $Mn^{3+}$ replaced with $Mn^{4+}$ for the electronic doping and providing potential charge carriers for the electronic conductivity in the double exchange mechanism. Following the considerable manganese perovskite in the optimized electronic doped range, our series of optimal doping manganese perovskite oxides samples $La_{0.7-x}Nd_xPb_{0.3}MnO_3$ ($x=0$, 0.05, and 0.1) were prepared by the sol–gel technique, in addition, by Nd doping, aimed at fine tuning the average A-site cation radius $\langle r_A \rangle$ in this series of manganese perovskite, $T_C$ were successfully modulated toward room temperature for the utility of this magnetocaloric effect [11,22–25]. Citric acid was used as gelling agents for $La^{3+}$, $Nd^{3+}$, $Pb^{2+}$, and $Mn^{3+/4+}$ ions in a sand bath, and the obtained gel was subjected to preparatory replacing of successive heat treatment at 873 K for 2 h. After that, the microcrystalline powder was pelletized, pressed into disks and successive sintered at 1573 K for 5 h in an oxygen flow. The crystal structure of the bulk samples was determined by an X-ray diffractometer (XRD) with Cu $K\alpha$ radiation (RK-D/Max-RA). $M$–$T$ and $M$–$H$ curves were measured by a vibrating sample magnetometer (VSM, LakeShore Cryotronics Inc.), with the sample placed inside a polyethylene pipe. Magnetization was measured using a vibrating sample magnetometer with an absolute accuracy of $5 \times 10^{-5}$ emu. The magnetization of an isothermal regime in the series samples was measured under an applied magnetic field varying from 0 to 9 kOe. The isotherms $M$ versus $H$ measurement was performed around the ferromagnetic ordering transition temperature ($T_C$) of the samples. In the vicinity of $T_C$, isothermal $M$–$H$ curves were obtained by a step of 5 K. The resistivity $\rho$ as a function of temperature was measured by the conventional in-line four-probe technique in a superconducting magnet with an applied field of 0 or 1 T.

## 3. Results and discussion

Fig. 1 shows the electrical resistivity and a colossal magnetoresistance as a function of temperature for the $La_{0.65}Nd_{0.05}Pb_{0.3}MnO_3$ sample at 0 and 1 T. Under 1 T magnetic field, there is suppressed resistivity behavior in the $La_{0.65}Nd_{0.05}Pb_{0.3}MnO_3$, which is a typical CMR behavior. The magnetoresistance was calculated according to the equation given below:

$$MR(\%) = \frac{\rho(H,T) - \rho(0,T)}{\rho(0,T)} \times 100\%$$

where $\rho(0,T)$ is the zero field resistivity and $\rho(H,T)$is the resistivity under external magnetic field.

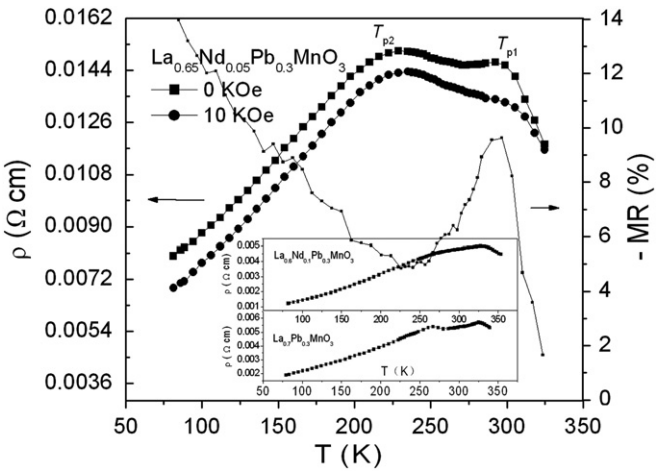


**Fig. 1.** Electrical resistivity as a function of temperature for the $La_{0.65}Nd_{0.05}Pb_{0.3}MnO_3$ sample under 0and 1 T and the its magnetoresistance calculated out. The inset shows the resistivity of $La_{0.7-x}Nd_xPb_{0.3}MnO_3$ ($x=0$ and 0.05) samples under 0 T as a function of temperature.

At $H=0$ T, the $La_{0.65}Nd_{0.05}Pb_{0.3}MnO_3$ sample showed the obvious double metal–insulator transition peaks where the first peak is at about 295 K defined as $T_{p1}$ and the second peak $T_{p2}$ is at around 225 K, and the maximum scale in the resistivity peaks $T_{p2}$ is larger than maximum scale in the resistivity peaks $T_{p1}$. These insets show the resistivity of $La_{0.7-x}Nd_xPb_{0.3}MnO_3$ ($x=0$ and 0.05) samples under 0 T as a function of temperature. Double metal–insulator peaks also occurred to these samples in the series.

Since the double metal–insulator transition peaks $T_{p1}$ and $T_{p2}$ occurred, double magnetic entropy change peaks or broaden magnetic entropy change in the manganese perovskite samples were expected in reason, which is rather attractive to improve the magnetocaloric effect and the magnetic refrigeration technology.

On one hand, the shifting of $T_{p1}$ to slightly higher temperatures in the presence of external magnetic field (Fig. 1) may be due to increased alignment of magnetic moments causing delocalization of '$e_g$' electrons and the enhancement of double exchange interaction between $Mn^{3+}$ and $Mn^{4+}$. The delocalization is suggested to contribute to the reduction of $T_{p1}$ resistivity peak. In addition, the fact that the negative colossal magnetoresistance peak was present in the vicinity of $T_{p1}$ for $x=0.05$ $La_{0.65}Nd_{0.05}Pb_{0.3}MnO_3$ (the right coordinate in Fig. 1) also indicates that the origin of both the negative colossal magnetoresistance and $T_{p1}$ peaks are related to the same mechanism, which is based on the double exchange interactions [26–29].

On the other hand, $T_{p2}$ peak does not shift on the resistivity curve plots along with the applied external magnetic field, which indicates that the origin of this peak is different from that of $T_{p1}$ peak. A previous study on $La_{2/3}Ca_{2/3}Mn_{1-x}Co_xO3$ suggested that the secondary $T_{p2}$ peak originates from oxygen vacancies due to substitution of trivalent $Co^{3+}$ in the place of $Mn^{4+}$ [28]. Mazaheri and Akhavan [26] suggested that the secondary $T_{p2}$ peak observed for $(La_{1-y}K_y)_{0.7}Ca_{0.3}MnO_3$ is related to large differences in the valence states and ionic radii of La, Ca, and K ions. Ibrahim suggested that secondary $T_{p2}$ peak observed for $La_{0.85-x}Sm_xAg_{0.15}MnO_3$ may possibly originate from the existence of mixed phases consisting of ferromagnetic and antiferromagnetic phases by increase of magnetic inhomogeneity as a result of double exchange interaction [21].

In a general way, the modification of La vacancies in the divalent alkali ions injection of $LaMnO_3$ stoichiometry phase, which is characterized by a long-range A-type antiferromagnetic order, is linked to superexchange between the $Mn^{3+}$ pairs with the

transition temperature $T_N$ of 140 K [30], which introduces $Mn^{4+}$ and results in the double exchange interaction that occurred between the moments of the $Mn^{4+}$ and those of its first $Mn^{3+}$ neighbors associated with $Mn^{3+}$–$Mn^{4+}$ pairs embedded in the $Mn^{3+}$–$Mn^{3+}$ antiferromagnetic matrix. The $Mn^{3+}$–$Mn^{4+}$ ferromagnetic cluster acts like an exchange between its neighboring top and down planes, whose moments point along the same direction as the net moment of the $Mn^{3+}$–$Mn^{4+}$ cluster does. It is also interesting to indicate the fact that the destabilization of the antiferromagnetic structure (measurable field variation of Curie temperature $T_C$ i.e. ferromagnetic ordering transition temperature) is related with the concentration of $Mn^{4+}$ due to La vacancies in the alkali ions substitution in part. The transport behavior in the perovskites is principally governed by ferromagnetic interactions of double exchange interaction origin pointing to a fast electron transfer between Mn ions [31]. It agrees with the general correlation between the strengths of the double exchange interaction and the structure of manganese perovskite (for example, the lattice parameters, the bond angle, the relative equilibrium bond lengths and the canted spin arrangement, the average A-site cation radius $\langle r_A \rangle$, the tolerance factor $t$) as well as the magnetic inhomogeneity, which is related with $Nd^{3+}$ doping in this series.

From the above-mentioned frame of reference, Song et al. suggested that $T_{p2}$ peak is related with the fact of the presence of ferromagnetic phase together with antiferromagnetic clusters below $T_C$ in Sm doped $La_{0.7-x}Sm_xSr_{0.3}MnO_3$ [32] and Cr doped $La_{2/3}Ca_{1/3}Mn_{1-x}Cr_xO_3$ [29], this thought is approved with the results of susceptibility measurements where the slope of the normalized $\chi$'versus temperature curve. It is possible that existence of antiferromagnetic clusters caused disconnectivity of the ferromagnetic phase contributing to the $T_{p2}$ peak. The second metal–insulator transition peaks may also be due to existence of ferromagnetic insulating clusters in the ferromagnetic metallic region below $T_C$, which may also contribute to electrical disconnectivity. Mixed ferromagnetic insulating and ferromagnetic metallic phases and resistivity increase at $T_{p2}$ have also been observed for $La_{1-x}Cd_xMnO_3$ [33] and $La_{0.9-x}Sm_xTe_{0.2}MnO_3$ [34]. Even more, Electron Paramagnetic Resonance study on $La_{0.875}Sr_{0.125}MnO_3$ has indicated the presence of mixed ferromagnetic insulating and ferromagnetic metallic phases below $T_C$ [35].

Fig. 2 shows the X-ray pattern of $La_{0.65}Nd_{0.05}Pb_{0.3}MnO_3$ and the compositions obtained crystallize in rhombohedral symmetry, and $R\bar{3}c$ space group in hexagonal setting was used for the profile matching; X-ray diffraction indicate that the sample is mainly composed of the perovskite phase, in addition, some peaks corresponding to MnO were also observed [PDF no. 77-2363 wavelength of 1.54 Å], since MnO exhibits antiferromagnetic behavior below $T_N = 116$ K and paramagnetic behavior above 116 K, its magnetic contribution to the magnetization of sample is negligible near room temperature [47]. The peak corresponding to $MnO_2$ and $Mn_3O_4$ is not observed from XRD. By the way, it can be concluded that the $T_{p2}$ peak is not due to impurity phases in the series samples, which is also approved by our XRD results [36].

The temperature dependence of low field magnetization for the sample $La_{0.65}Nd_{0.05}Pb_{0.3}MnO_3$, shown in Fig. 3, was measured in a scheduled range of temperature (from 220 up to 370 K) in 1 kOe applied field in order to determine the transition temperature of the material. The ferromagnetic ordering transition temperature $T_C$, defined as the temperature at which the $\partial M/\partial T$–$T$ curve reaches a minimum, had been determined from the $M$–$T$ curves. Fig. 4 shows the plots of magnetization against applied field obtained at various temperatures for the sample of $La_{0.65}Nd_{0.05}Pb_{0.3}MnO_3$. In our experiments, the changing rate of applied field (22 Oe/s) is slow enough to get an isothermal $M$–$H$ curve.

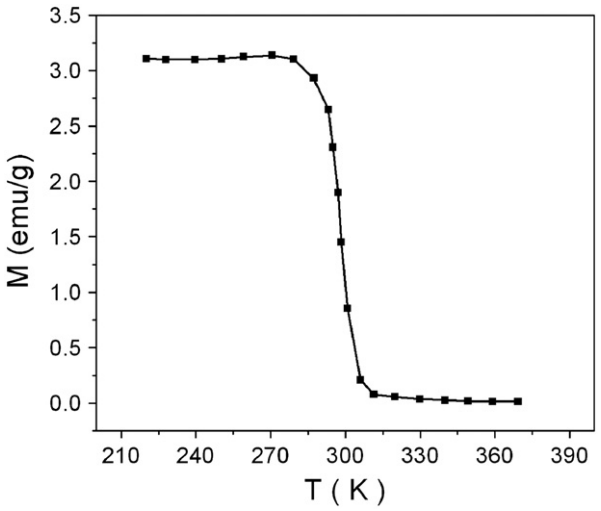


**Fig. 3.** Temperature dependence at 1 kOe low field magnetization for sample $La_{0.65}Nd_{0.05}Pb_{0.3}MnO_3$.

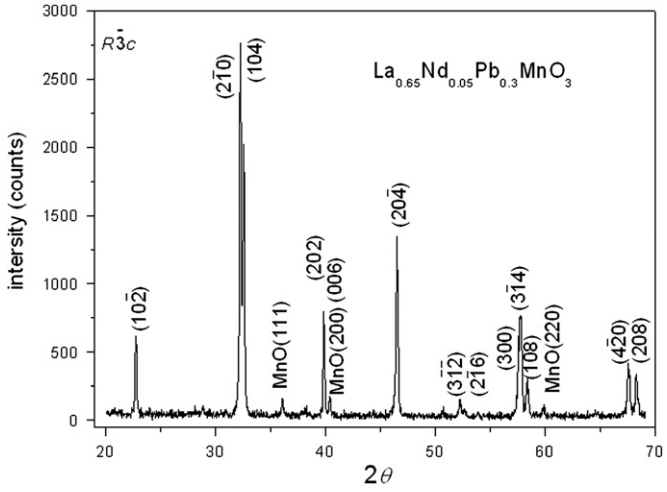


**Fig. 2.** X-ray diffraction patterns of the $La_{0.65}Nd_{0.05}Pb_{0.3}MnO_3$ sample. Indexing is in hexagonal setting.

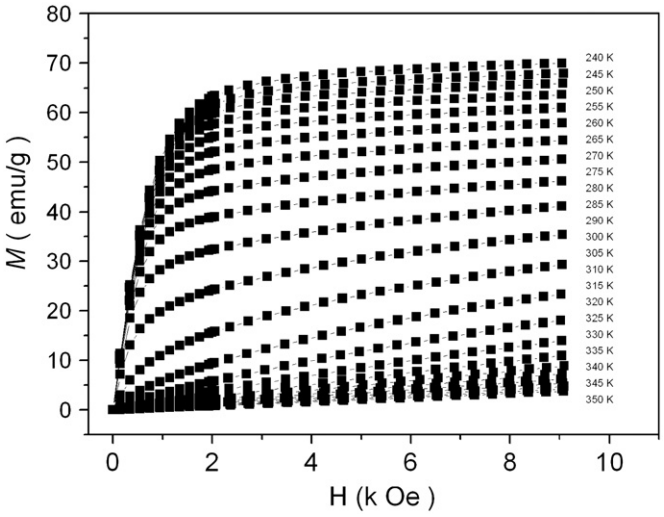


**Fig. 4.** Isothermal magnetizations of sample as a function of applied magnetic field at different temperatures for $La_{0.65}Nd_{0.05}Pb_{0.3}MnO_3$. The temperature step is 5 K in the region near Curie temperature from 240 to 350 K.

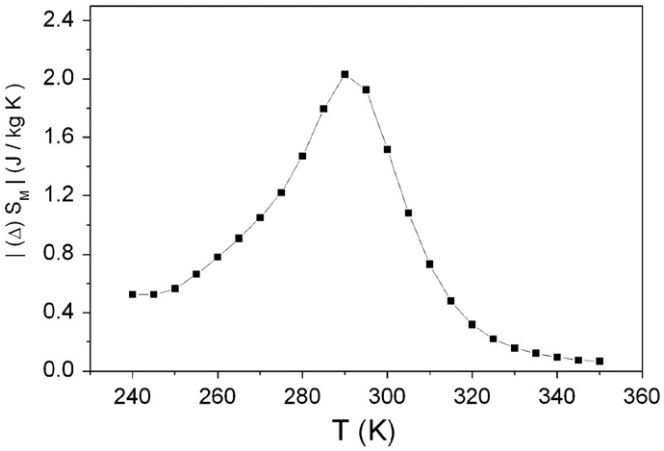


**Fig. 5.** Magnetic entropy changes of $La_{0.65}Nd_{0.05}Pb_{0.3}MnO_3$ sample at a magnetic field $H=9$ kOe as a function of temperature.

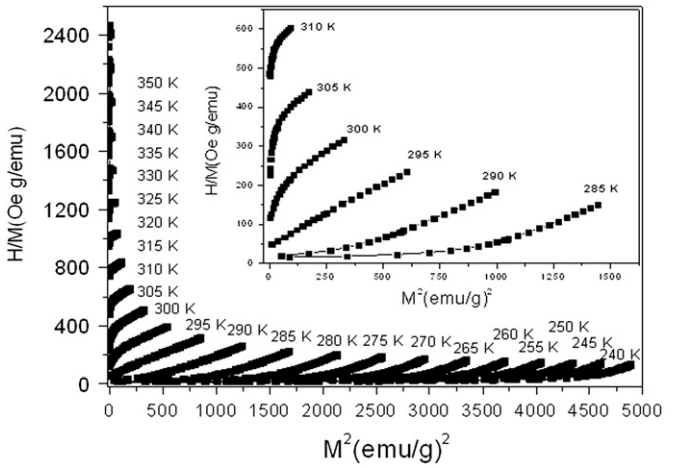


**Fig. 6.** $H/M$ versus $M^2$ plots of isotherms around Curie temperature, the inset clearly shows the slope of isotherm plots from the negative sign to the positive sign for some temperatures.

The magnetic entropy change, which results from the spin-ordering (i.e. ferromagnetic ordering) and is induced by the variation of the applied magnetic field from 0 to $H_{max}$, is given by

$$\Delta S_H = \sum_i \frac{M_i - M_{i+1}}{T_{i+1} - T_i} \Delta H_i$$

Fig. 5 shows the temperature dependence of magnetic entropy change for sample $La_{0.65}Nd_{0.05}Pb_{0.3}MnO_3$. The peak of magnetic entropy changes of the sample is around each Curie temperature $T_C$. It is clear that the magnetic entropy change in the series originates from the considerable change of magnetization near $T_C$. The maximum entropy change $\Delta S_H$corresponding to a magnetic field variation of 9 kOe for $La_{0.65}Nd_{0.05}Pb_{0.3}MnO_3$ is about $-2.03$ J/kg K at 290 K.

From a cooling perspective, it is important to consider not only the magnitude of the magnetic entropy change but also the refrigerant capacity *RC*, which depends on both the magnetic entropy change and its temperature dependence.

The magnetic cooling efficiency of a magnetocaloric material can be, in simple cases, evaluated by considering the magnitude of $\Delta S_H$ and its full-width at half maximum ($\delta T_{FWHM}$) [11,37–38]. It is easy to establish the product of the $\Delta S_H$ maximum and the full-width at half maximum ($\delta T_{FWHM} = T_2 - T_1$) as

$$RCP = -\Delta S_H(T,H)\delta T_{FWHM}$$

where *RCP* stands for the so-called relative cooling power based on the magnetic entropy change. For the sample of $La_{0.65}Nd_{0.05}Pb_{0.3}MnO_3$, 71.05 J/kg *RCP* is figured out corresponding to a magnetic field variation of 9 kOe.

In addition, the thermal and field hysteresis losses in magnetocaloric materials should also be considered in materials with first-order magnetic phase transitions especially in high magnetic field. The field hysteresis losses cost in energy to make one cycle of the magnetic field when calculating *RC* of a magnetic refrigerant material being subjected to field cycling. It had been calculated that the influence of hysteretic losses is small in the perovskites manganites material at 9 kOe magnetic field and *RCP* is approximately close to *RC* with thermal/field hysteresis losses [39].

To characterize the first-order or second-order phase transition, the purely magnetic ways to determine are the Banerjee criteria in 1964, in which by analyzing $H/M$ versus $M^2$ curves Banerjee detected the essential similarity between the Laudau–Lifshitz and the Bean–Rodbell criteria and condensed them into one that provides a tool to distinguish first-order magnetic transitions from second-order ones. It consists of the observation of the slope of isotherm plots of $H/M$ versus $M^2$. Fig. 6 shows $H/M$ versus $M^2$ plots of Fig. 4 isotherms in the vicinity of the Curie temperature. It is clear that these plots of inset show from the negative sign to the positive sign for some temperatures, which indicate that this phase transition is a first-order phase transition, in contrast to the slope sign in the invariable positive denoting the second-order character of the phase transition [40–41].

$Nd^{3+}$ possesses a smaller radius than $La^{3+}$, the substitution of $Nd^{3+}$ for partial $La^{3+}$ can lead to the decrement of average A-site cation radius $\langle r_A \rangle$ and tolerance factor *t*, which distorts the original cubic structure and adjusts Mn–O bond length and Mn–O–Mn bond angle. For the above reasons, the ferromagnetic coupling is weakened, and thus the magnetocaloric effect is weakened [5]. $Nd^{3+}$ differs from $La^{3+}$ and possesses spin system itself. The contributions of Nd spin system to the entropy are introduced in this perovskite manganite material system with two spin systems. In addition, the interactions between the Mn and Nd spin systems may have some effects on the entropy, the above-mentioned factors lead to additional magnetic entropy change and favor magnetocaloric effect [42,43]. However, the magnetocaloric effect is principally governed by ferromagnetic interactions of double exchange interaction in the series, with the increase of $Nd^{3+}$ doped amount, which decreases the average A-site cation radius $\langle r_A \rangle$ and tolerance factor *t*, increases the Jahn–Teller deformation, gradually weakens the double exchange interaction, then the magnetocaloric effect drop into the shade after going through the maximum magnetic entropy change [10–11,44–46].

## 4. Conclusion

For the sample $La_{0.65}Nd_{0.05}Pb_{0.3}MnO_3$ with the double metal–insulator peaks, $T_{p1}$ and $T_{p2}$, the double peaks of the maximum magnetic entropy change did not occurred. Our results showed that $T_{p1}$, which coincides with $T_C$, is related to the double exchange mechanism as it was affected by external magnetic field and was also accompanied by a colossal magnetoresistance peak. $T_{p2}$ peak changed weakly in external magnetic field and is suggested to be due to the coexistence of ferromagnetic, paramagnetic or antiferromagnetic clusters in the ferromagnetic metallic region, the single peaks of the magnetocaloric effect originated from the differential coefficient of magnetic moment to temperature. The possibility of faint magnetic inhomogeneity mixed in the double exchange strong magnetic signal results in this relatively well refrigerant capacity around room temperature.

## References


[1] S Jin, T.H Tiefel, M McCormack, R.A Fastnacht, R Ramesh, L.H Chen, Science 264 (1994) 413.
[2] C.N Rao, B Raveau, Colossal Magnetoresistance, Charge Ordering and Related Properties of Manganese Oxides, World Scientific, Singapore, 1998.
[3] Y Tokura, T Tomioka, J. Magn. Magn. Mater. 200 (1999) 1.
[4] J. Fontcuberta, B. Martinez, A. Seffar, S. Pinol, J.L. Garcia-Munoz, X. Obradors, Phys. Rev. Lett. 76 (1996) 1122.
[5] P.G. Radaelli, G. Iannone, M. Marezio, H.Y. Hwang, S-W. Cheong, J.D. Jorgensen, D.N. Argyriou, Phys. Rev. B 56 (1997) 8265.
[6] A.J. Millis, Nature 392 (1998) 147.
[7] H. Roder, Jun Zang, A.R. Bishop, Phys. Rev. Lett. 76 (1996) 1356.
[8] H.Y. Hwang, S-W Cheong, P.G. Radaelli, M. Marezio, B. Batlogg, Phys. Rev. Lett. 75 (1995) 914.
[9] Z.B. Guo, Y.W. Du, J.S. Zhu, H. Huang, W.P. Ding, D. Feng, Phys. Rev. Lett. 78 (1997) 1142.
[10] E Dagotto, T. Hotta, A. Moreo, Phys. Rep. 344 (2001) 1.
[11] M.H. Phan, S.C. Yu, J. Magn. Magn. Mater. 308 (2007) 325.
[12] C. Zener, Phys. Rev 81 (1951) 440;
C. Zener, Phys. Rev. 82 (1951) (1951) 403.
[13] D.T. Morelli, A.M. Mance, J.V. Mantese, A.L. Micheli, J. Appl. Phys. 79 (1996) 373.
[14] Y. Sun, X.J. Xu, Y.H. Zhang, Magn. Magn. Mater. 219 (2000) 183.
[15] X.X. Zhang, J. Tejada, Y. Xin, G.F. Sun, K.W. Wong, X. Bohigas, Appl. Phys. Lett. 69 (1996) 3596.
[16] W. Zhong, W. Chen, W.P. Ding, N. Zhang, A. Hu, Y.W. Du, Q.J. Yan, Magn. Magn. Mater. 195 (1999) 112.
[17] X. Bohigas, J. Tejada, M.L. Marinez-Sarrion, S. Ttipp, R. Black, Magn. Magn. Mater. 208 (2000) 85.
[18] J. Mira, J. Rivas, L.E. Hueso, F. Rivadulla, M.A.Lopez Quintela, J. Appl. Phys. 91 (2002) 8903.
[19] S.M. Yusuf, J.M. De Teresa, P.A. Algarabel, J. Blasco, M.R. Ibarra, Amit Kumar, C. Ritter, Physica B 385–386 (2006) 401.
[20] B.F. Yu, Q. Gao, B. Zhang, X.Z. Meng, Z. Chen, Int. J. Refrig. 26 (2003) 622.
[21] N. Ibrahim, A.K. Yahya, S.S. Rajput, S. Keshri, M.K. Talari, J. Magn. Magn. Mater. in press, doi: 10.1016/j.jmmm.2011.03.027 (accessed 25.03.11).
[22] Z.M. Wang, Q.Y. Xu, J.Z. Sun, J. Pan, H. Zhang, Phys. B: Condens. Matter 406 (2011) 1436.
[23] Z.M Wang, T. Tang, Y.P. Wang, S.Y. Zhang, Y.W. Du, J. Magn. Magn. Mater. 246 (1–2) (2002) 254.
[24] Z.M. Wang, G. Ni, Q.Y. Xu, H. Sang, Y.W. Du, J. Magn. Magn. Mater. 234 (2001) 371.
[25] ZM. Wang, G. Ni, Q.Y. Xu, H. Sang, Y.W. Du, J. Appl. Phys. 90 (2001) 5689.
[26] M. Mazaheri, M. Akhavan, Physica B 405 (2010) 72.
[27] T.S. Zhao, B.H. Li, H. Han, J. Magn. Magn. Mater. 320 (2008) 924.
[28] Qianying Yu, Jincang Zhang, Rongrong Jia, Chao Jing, Shixun Cao, J. Magn. Magn. Mater. 320 (2008) 3313.
[29] X. Xiao, S.L. Yuan, Y.Q. Wang, G.M. Ren, J.H. Miao, G.Q. Yu, Z.M. Tian, L. Liu, L. Chen, S.Y. Yin, Solid State Commun. 141 (2007) 348.
[30] C. Ritter, M.R. Ibarra, J.M. De Teresa, P.A. Algarabel, C. Marquina, J. Blasco, J. Garcia, S. Oseroff, S.W. Cheong, Phys. Rev. B 56 (1997) 8902.
[31] J. Topfer, J.B. Goodenough, Chem. Mater. 9 (1997) 1467.
[32] SONG Qixiang, WANG Guiying, YAN Guoqing, MAO Qiang, WANG Wengi, PENG Zhensheng, J. Rare Earths 26 (2008) 821.
[33] G.N. Rao, R.C. Saibal Roy, Yang, J.W. Chen, J. Magn. Magn. Mater. 260 (2003) 375.
[34] G.H. Zheng, Z.X. Dai, Y.Y. Zhang, Y.P. Sun, J. Alloys Compd. 489 (2010) 348.
[35] Shiming Zhou, Lei Shi, Jiyin Zhao, Haipeng Yang, Lin Chen, Solid State Commun. 142 (2007) 634.
[36] Guerman Popov, Jacob Goldsmith, Martha Greenblatt, J. Solid State Chem. 175 (2003) 52.
[37] V.K. Pecharsky, K.A. Gschneidner, A.O. Tsokol, Rep Prog. Phys 68 (2005) 1479.
[38] V.K. Pecharsky, K.A Gschneidner, Annu. Rev. Mater. Sci. 30 (2000) 387.
[39] N.S. Bingham, M.H. Phan, H. Srikanth, M.A. Torija, C. Leighton, J. Appl. Phys. 106 (2009) 023909.
[40] B.K. Banerjee, Phys. Lett. 12 (1964) 16.
[41] J. Mira, J. Rivas, F. Rivadulla, C. Vazquez-Vazquez, M.A. Lopez-Quintela, Phys. Rev. B 60 (1999) 2998.
[42] J.E. Gordon, R.A. Fisher, Y.X. Jia, N.E. Phillips, S.F. Reklis, D.A. Wright, A. Zettl, Phys. Rev. B 59 (1999) 127.
[43] J.E. Gordon, R.A. Fisher, Y.X. Jia, N.E. Phillips, S.F. Reklis, D.A. Wright, A. Zettl, J. Magn. Magn. Mater. 177–181 (1998) 856.
[44] J.B. Goodenough, J.M. Lango, Landolt Boornstein Tabellen New Series, II/4a, Springer, Berlin, 1970, p. 231.
[45] A. Szewczyk, H. Szymczak, A. Wisniewski, K. Piotrowski, R. Kartaszynski, Appl. Phys. Lett. 77 (2000) 1026.
[46] V.K. Pecharsky, K.A. Gschneidner, J. Magn. Magn. Mater. 200 (1999) 44.
[47] 〈http://en.wikipedia.org/wiki/N%C3%A9el_temperature〉.